Boson enhancement of finite-temperature coherent dynamics for deuterium in metals

K. B. Whaley
Department of Chemistry, University of California, Berkeley, California 94720
(Received 3 October 1989)

Effects of coherent many-particle dynamics in providing local site density fluctuations at finite temperatures for hydrogen isotopes in metals are analyzed with tight-binding calculations based on a Hubbard Hamiltonian. These fluctuations increase with temperature, with average deuterium density, and with the magnitude of the site-to-site tunneling. Consequences of such density fluctuations for deuterium dynamics at high concentrations are evaluated within a self-consistent formulation for self-screening of the deuteron-deuteron interaction. This leads to a prediction of significant enhancement of diffusion at high concentration for bosonic species, and anomalous isotope effects for hydrogen diffusion. Extrapolation to the nuclear regime yields estimates of finite-temperature bosonic collective effects on the nuclear reaction rate between deuterons in stoichiometric PdD, yielding rates which are several orders of magnitude below recent experimentally inferred values.

I. INTRODUCTION

Dynamics of hydrogen isotopes in metals is dominated by quantum transport, with phonon-assisted tunneling providing the primary mechanism for mobility below about 500 K.[1] For low concentrations, small polaron theory, modified to treat light interstitial atomic species rather than electrons, yields a qualitative (and for bcc metals also a quantitative) understanding of diffusion rates. At high concentrations however, there exist only scant experimental data on the dynamical behavior. Even less theoretical understanding exists, there being no analogue of the polaron theories for many, strongly interacting, tunneling interstitials. Unusual isotopic anomalies measured in the surface diffusion of hydrogen on tungsten[2] have suggested that *at high concentrations,* where a single-particle description of the dynamics is not valid,[3] collective quantum-statistical effects may influence the many-body tunneling dynamics.[2,4] Recent experimental and theoretical interest in the dynamics of hydrogen isotopes in metals has been renewed by experimental claims of evidence for unprecedented enhancements of the nuclear fusion reaction $d+d\rightarrow{}^3\mathrm{He}+n$ in palladium, at high concentrations of deuterium.[5,6] Experimental verification of these results has so far proven ambiguous.[7] The initially reported fusion rates of $\sim 10^{-23}$ fusion events/(deuteron pair s) (Ref. 6) represent a significant increase over the intrinsic fusion rate of $\sim 10^{-74}$/(deuteron pair s) in isolated ground state D_2,[8] although they are still considerably below the values of $\sim 10^{11}$/(deuteron pair s) achieved for muon-catalyzed fusion.[8-10] One possible reason for such an enhancement could be a bosonic collective effect, of which the simplest is an efficient collective self-screening of the Coulomb barrier. We investigate here the quantum collective effects peculiar to deuterium in metallic environments, and estimate the maximum effect these can have, both on the diffusional dynamics, and on a $d+d$ nuclear reaction in palladium at finite temperatures.

We shall treat the dynamics of interstitial hydrogen isotopes with a generalized Hubbard Hamiltonian model,[4] acting on states of spin-$\frac{1}{2}$ particles (fermions) for hydrogen and tritium, and on states of spin-1 particles (bosons) for deuterium. This model contains the most important physics for the hydrogen dynamics at high concentrations, namely a single-particle site-to-site tunneling term (t), and a site-localized interaction term (U). The choice of statistics corresponds to the ionized form of the interstitial. This is the most appropriate choice in metals, since although static-charge-density calculations show apparently normal screening-charge distributions around the proton/deuteron nuclei,[11] dynamic electronic properties clearly indicate that the dynamics correspond to those of ionized species.[12] Note that, since hydrogen mobility in metals is a phonon-assisted tunneling process, the relevant tunneling amplitudes at finite temperature may be considerably larger than those between ground vibrational states.[1,13] We demonstrate below that collective coherent dynamical effects are strongly magnified by increasing either temperature or the magnitude of the tunneling amplitude, t. Leggett and Baym have recently calculated an exact upper bound of $\sim 3\times 10^{-47}/\mathrm{s}^{-1}$ for the fusion rate of two deuterons in palladium at zero temperature.[14] Their theory is valid for any number of deuterons, and correctly takes collective Bose effects at $T=0$ into account, but does not allow for collective effects at finite temperatures. In this paper we make estimates of the $d+d$ fusion-rate enhancements, due to finite-temperature Bose effects in the metallic environment, constructed within a theory which allows the maximum possible effects of coherence.

In Sec. II we describe the Hubbard model for interstitial dynamics, present calculations of the local site density fluctuations and estimate maximal values of these for deuterium in palladium. A self-consistent theory for self-screening of the deuteron-deuteron interaction and enhancement of this due to the boson statistics is given in Sec. III. We show how this will affect the short-range part of the potential affecting diffusional dynamics at high concentrations. Extrapolation down to nuclear di-

mensions yields a contribution to screening of the internuclear Coulomb barrier at short distances, and this is then used in Sec. IV to obtain estimates of the rate of $d+d$ fusion in palladium, as a function of the Hubbard parameters U and t.

II. GENERALIZED HUBBARD MODEL

A. Hubbard Hamiltonian model for coherent interstitial motion at high concentrations

For particles of general spin s with projections σ, the Hubbard Hamiltonian with on-site repulsive interactions is given by

$$\mathcal{H}=(-t)\sum_{\substack{\langle ij\rangle \\ \sigma}} c_{i\sigma}^{\dagger}c_{j\sigma}+\tfrac{1}{2}U\sum_{\substack{i \\ \sigma\sigma'}} c_{i\sigma}^{\dagger}c_{i\sigma'}^{\dagger}c_{i\sigma'}c_{i\sigma} \tag{1}$$

where t is the single-particle intersite tunneling term between nearest-neighbor sites ij, and U the two-particle intrasite repulsion. Hence $c_{i\sigma}$ ($c_{i\sigma}^{\dagger}$) is the annihilation (creation) operator for a particle of spin s, and z component σ, located at site i. Although the Hamiltonian is identical for fermions and bosons, its effect on many-body states is very different. The eigenstates in small periodic clusters and delocalization properties of these were recently investigated by us for spin-$\frac{1}{2}$ fermions, and spin-0 and spin-1 bosons.[4] We use the same periodic-cluster technique here to evaluate single-site density fluctuations for particles with spin $\frac{1}{2}$ and 0. Our previous work showed that the differences between statistics, rather than the magnitude of the spin, are important,[4] so we restrict ourselves here to the computationally simpler case of spin 0 for deuterium.

In the finite-cluster method,[15] the Hamiltonian matrix for n particles on an N-site cluster is constructed explicitly in a localized spin-space basis. Since the Hamiltonian commutes with the total cluster spin S and its projection S_z, we project the many-body states onto a particular (S,S_z) subspace and solve for one value of S_z only. [Using spin-0 bosons yields a subspace isomorphic to the $(S_m,S_z=S_m)$ subspace, where S_m is the maximum cluster spin obtained for spin-1 bosons.] When periodic boundary conditions are imposed on the cluster, the many-body states are also eigenstates of total K, thereby yielding a finite discrete sampling of the Brillouin zone.

We consider here two clusters for hydrogen isotopes in palladium, chosen to represent two regions differing in the range of coherent tunneling allowed. The first cluster is a four-site cluster, consisting of, e.g., four interconnected octahedral sites in the Pd fcc lattice (Fig. 1). In this highly connected cluster, each site is connected to all three other inequivalent sites, and the effect of the tunneling term t is therefore enhanced. The second cluster is a two-site (degenerate) cluster, representing, e.g., two octahedral sites, or two tetrahedral sites. A two-site cluster calculation is important since at room temperature the extent of coherent tunneling motion is expected to be limited to nearest-neighbor sites,[1] with only small contributions from the longer-range coherences contained in the four-site model. Calculations are performed both with and without periodic boundary conditions, for similar reasons, namely with and without long-range single-particle coherences included.

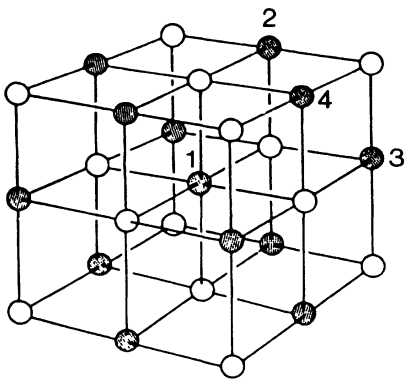

FIG. 1. Cluster of face-centered cubic Pd containing $N=4$ octahedral sites. Pd sites are indicated by open circles, and the interstitial octahedral sites by solid circles. The four inequivalent sites are labeled 1–4.

B. Site density fluctuations

Table I lists the total number of many-body states for occupancies $n=1$ to $n=2N$ of the N-site clusters, for $N=2$ and 4. We define the local site density fluctuation by

$$\langle(\delta n)^2\rangle=\langle\overline{n_1^2}\rangle-\langle\overline{n_1}\rangle^2$$

where

$$\overline{n}_1=\frac{1}{N}\sum_i n_i,\quad \overline{n_1^2}=\frac{1}{N}\sum_i n_i^2\ , \tag{2}$$

and $\langle\ \rangle$ denotes a thermal average. Here $\overline{n}_1$ is the site-averaged number operator for one site in the N-site cluster, and $\overline{n_1^2}$ is the site average of n_i^2. Once the eigenstates of H have been determined for n particles on an N-site cluster, $\langle(\delta_n)^2\rangle$ is evaluated within the canonical ensemble at temperature T. $\langle(\delta n)^2\rangle$ thus contains both a thermal average over the many-body states, and a site

TABLE I. Total number of many-body states for $N=2$ and $N=4$ site clusters with n particles.

	n	$S=0$	$S=\frac{1}{2}$
$N=2$	1	2	4
	2	3	6
	3	4	4
	4	5	1
$N=4$	1	4	8
	2	10	28
	3	20	56
	4	35	70
	5	56	56
	6	84	28
	7	120	8
	8	165	1

average over all sites i in the cluster. It is a measure of the temperature-dependent density susceptibility within the cluster, i.e., of the local-density fluctuations possible on each site, within the constraint of a constant cluster occupancy of n particles on N sites.

Figures 2 and 3 show the behavior of $\langle(\delta n)^2\rangle$ as a function of n, for spin-$\frac{1}{2}$ fermions and spin-0 bosons, at various ratios of U/t on the four-site cluster. Periodic boundary conditions were employed here. At all conditions, and at all temperatures, we see that the density fluctuations are larger for bosons, and generally become increasingly so as (i) concentration (n/N) increases, (ii) the tunneling amplitude t increases, or (iii) temperature increases. At double-site occupancy, $n=2N$, the fermion fluctuations are zero as a consequence of Pauli exclusion, while the boson fluctuations continue to increase with density. This effect is most marked at high temperatures, and also for $U=0$ [Fig. 3(a)]. Even in this limit however, the increase of $\langle(\delta n)^2\rangle$ with n is considerably suppressed relative to a free, ideal Bose-Einstein gas,[16] reflecting the tight-binding nature of the motion. As temperature decreases, relative to U, the magnitude of average fluctuations decreases, even leading to a local minimum for bosons at single-site occupancy, $n=N$ [Figs. 2(c), 3(b), and 4(b), 4(c)]. The general conclusion is that as long as t is finite, small nonzero site density fluctuations are possible at full coverage, and are significantly greater than the corresponding fluctuations allowed in the atomic limit ($t=0$). [Compare Figs. 2(b) and 3(b).]

Figure 4 shows $\langle(\delta n)^2\rangle$ for the two-site cluster, evaluated without periodic boundary conditions. Similar behavior is seen as in Figs. 2 and 3, with the absolute magnitude of $\langle(\delta n)^2\rangle$ decreased throughout. This reflects the reduced contribution of coherent single-particle motion (t) to enabling local site fluctuations. Note that with $N=2$ sites, large fluctuations are apparent for coverage $n=3$ as well as $n=1$. This is due to the degeneracy of states with either one or two particles on each site, and is

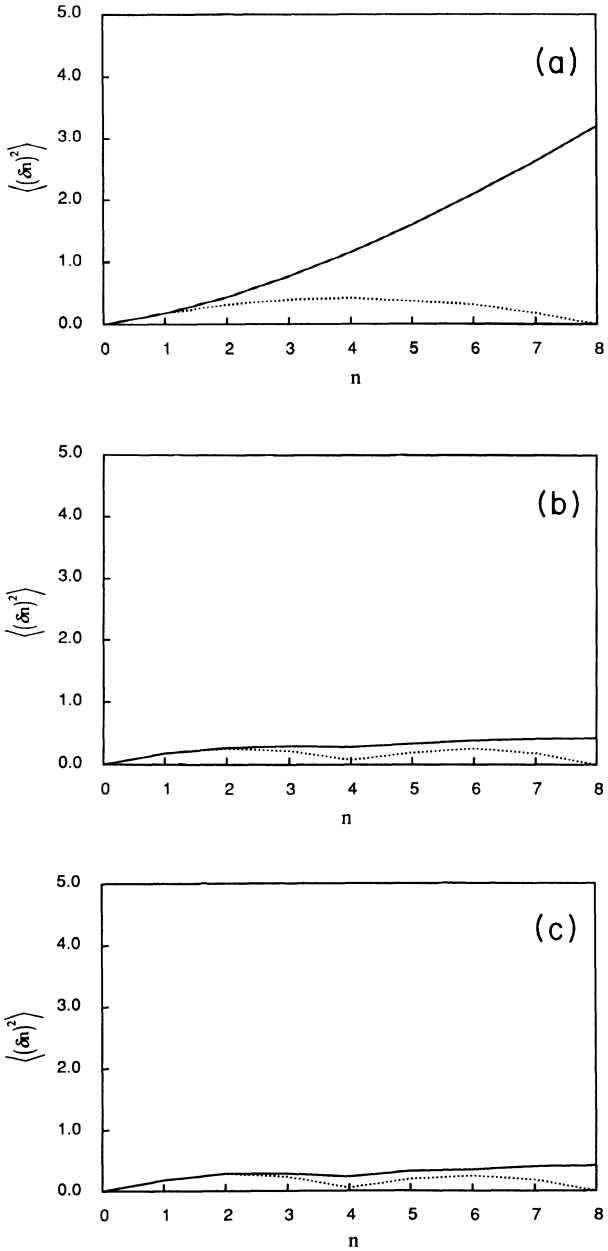

FIG. 2. $\langle(\delta n)^2\rangle$ for bosons (——) and fermions (· · · ·) in the ($N=4$)-site cluster with periodic boundary conditions, for the parameter ratio $U/t=36$, at temperatures (a) $k_BT=1000t$, (b) $k_BT=10t$, (c) $k_BT=t$.

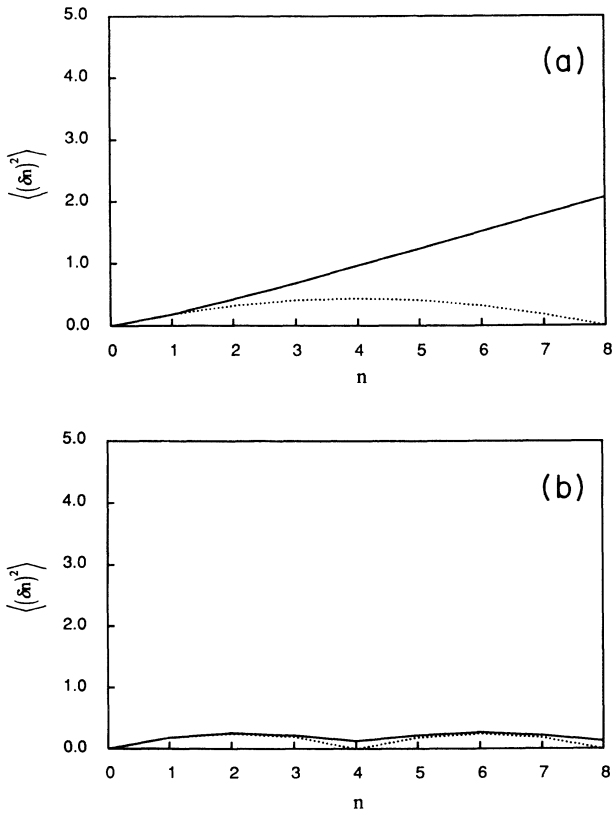

FIG. 3. $\langle(\delta n)^2\rangle$ for bosons (——) and fermions (· · · ·) in the ($N=4$)-site cluster with periodic boundary conditions, with (a) $U=0$, $t=1$, $k_BT=10t$, and (b) $t=0$, $U=36$, $k_BT=10$.

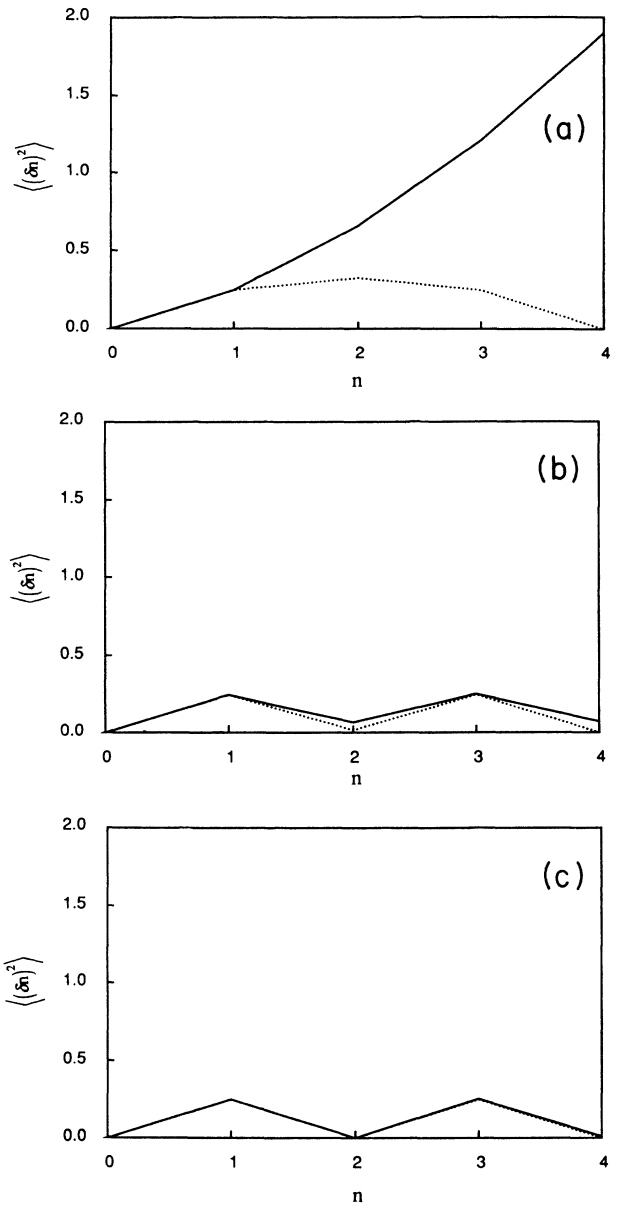

FIG. 4. $\langle(\delta n)^2\rangle$ for bosons (——) and fermions (· · · ·) in the ($N=2$)-site cluster without periodic boundary conditions, for the parameter ratio $U/t=36$, at temperatures (a) $k_BT=1000t$, (b) $k_BT=10t$, (c) $k_BT=t$.

particular to the $N=2$ cluster.

A conservative estimate of $\langle(\delta n)^2\rangle$ for deuterium in palladium may be obtained by adapting typical values of the Hubbard t and U parameters for interstitial hydrogen in metals, to palladium. Estimates of t in metals range from $\sim 10^{-6}$ to ~ 1 meV in ground vibrational states of H, and up to ~ 16 meV for low-lying excited states.[1] The values of t which will be appropriate at room temperature will be primarily those for excited vibrational states of H, as inspection of the potential energy profile for the octahedral-tetrahedral-octahedral tunneling path for H in palladium shows.[13] Thus as an initial estimate, we take $t\sim 1$ meV for D in Pd. For interstitial hydrogenic species, the repulsion U is a complex parameter expressing the overall repulsive energy between the nuclei, and their associated electron distributions in the metal environment, and thus really corresponds to a screened Hubbard U. U will in general also be dependent on the vibrational level. In principle U could be obtained from *ab initio* calculations. Recently several such calculations have been made for the binding energy of two deuterium atoms in an octahedral site.[17–19] The results of Ref. 19 allow us to extract an estimate of ~ 3 eV for the energy,

$$U\sim E_{\rm tot}({\rm Pd}_n{\rm H}_{n+1})-E_{\rm tot}({\rm Pd}_n{\rm H}_n)-E_{\rm binding}\quad ({\rm H\ in\ PdH}) \qquad (3)$$

for taking two hydrogen interstitials from different octahedral sites and placing them on the same site. We use this here as an estimate of U in the absence of a full *ab initio* calculation, bearing in mind that U may actually vary from 1 to 10 eV. A complete temperature-dependent theory would require a multiband Hubbard calculation, with band-dependent U and t parameters as noted above. Longer-range interactions may also play a role.[20] However, we expect that the gross dependence on the Hubbard parameters (which are not accurately known), and order of magnitude estimates can be satisfactorily obtained from a single-band theory. Table II then shows $\langle(\delta n)^2\rangle$ for D (bosons) in Pd, with $U/t=10^2$, 10^3, 10^4 and $k_BT/t=1$–25. Both single-site occupancy, $n=N$ (PdD), and double-site occupancy, $n=2N$ (PdD_2) values are shown. Entries in the first, fourth, and fifth rows correspond to $t=1$ meV, $k_BT=25$ meV (room temperature), and U varying from 0.1 to 10

TABLE II. $\langle(\delta n)^2\rangle$ for d^+ (bosons) in Pd, evaluated for (a) ($N=4$)-site clusters with periodic boundary conditions, and (b) ($N=2$)-site clusters without periodic boundary conditions. Integers in parentheses refer to the power of 10.

		$N=2$		$N=4$	
U/t	k_BT/t	$n=2$	$n=4$	$n=4$	$n=8$
10^2	25	0.33(−1)	0.36(−1)	0.11	0.16
10^2	10	0.59(−3)	0.18(−2)	0.30(−1)	0.10
10^2	1	0.40(−3)	0.12(−2)	0.29(−1)	0.10
10^3	25	0.40(−5)	0.12(−4)	0.20(−3)	0.62(−3)
10^4	25	0.00	0.00	0.20(−5)	0.60(−5)
10^2	0	0.40(−3)	0.12(−2)	0.29(−1)	0.10
10^3	0	0.40(−5)	0.12(−4)	0.20(−3)	0.62(−3)
10^4	0	0.00	0.00	0.20(−5)	0.60(−5)

eV. The second row corresponds to parameters $U=0.25$ eV, $t=2.5$ meV, $k_B T=25$ meV, and the third row to $U=2.5$ eV, $t=25$ meV, $k_B T=25$ meV. For comparison, the sixth, seventh, and eighth rows show the corresponding values of $\langle(\delta n)^2\rangle$ at $T=0$, i.e., in the ground state, for $U/t=10^2$, 10^3, and 10^4, respectively.

The results shown in Figs. 2–4 and Table II clearly show enhancement of the local site density fluctuations for bosonic interstitial species. The magnitude of these density fluctuations for a given size cluster is greater when periodic boundary conditions are imposed. The fluctuations exist at room temperature, despite an unfavorable on-site repulsion energy U, because of the small but non-negligible contribution from coherent tunneling motion, and are considerably larger than the values at $T=0$. This indicates that a large apparent repulsive energy between two deuterium species in one site does not necessarily mean that such configurations are impossible at room temperatures.

III. SELF-CONSISTENT BOSON SCREENING OF DEUTERIUM IN METALS

In the Hubbard description, Coulombic interactions of d^+ with d^+ are subsumed into U, and the collective motion of the d^+ species is given by the Hubbard tight-binding dynamics. An approximate, self-consistent theory of the effective d^+-d^+ interaction can be obtained within linear response, treating the response of electrons and the Hubbard-screened d^+ species independently. Thus the effective potential at r due to a charge Q at the origin is given by

$$V_{\text{eff}}(r)=\frac{Q}{r}-\int\int d\mathbf{r}'d\mathbf{r}''\frac{e}{|\mathbf{r}-\mathbf{r}'|}\chi_e(\mathbf{r}'\mathbf{r}'')eV_{\text{eff}}(r'') - \int\int d\mathbf{r}'d\mathbf{r}''\frac{e}{|\mathbf{r}-\mathbf{r}'|}\chi_d(\mathbf{r}'\mathbf{r}'')eV_{\text{eff}}(r'') , \quad (4)$$

where χ_e and χ_d are the density-density susceptibilities of the electrons and of the Hubbard d^+ species in the metal, respectively. In such a self-consistent formulation, the Hubbard parameter U, which determines χ_d, is not independent of $V_{\text{eff}}(r)$. Equation (4) could thus, in principle, be used to self-consistently determine these quantities, provided the electronic interactions were also well characterized. Within the present aim of understanding the maximal effects of $\langle(\delta n)^2\rangle$, we neglect this interdependence, and consider U, and hence χ_d, as independent variables determining $V_{\text{eff}}(r)$. Fourier transforming Eq. (4), we obtain then

$$\hat{V}_{\text{eff}}(\mathbf{k})=\frac{4\pi Q}{k^2\epsilon(\mathbf{k})} , \quad (5)$$

$$\epsilon(\mathbf{k})=1+4\pi\frac{e^2}{k^2}[\hat{\chi}_e(\mathbf{k})+\hat{\chi}_d(\mathbf{k})] \quad (6)$$

with

$$\hat{\chi}(\mathbf{k})=\beta\langle n_{-\mathbf{k}};n_{+\mathbf{k}}\rangle , \quad (7)$$

i.e., the Fourier transform of the symmetrized density-density susceptibility. The behavior of the electronic contribution to $V_{\text{eff}}(r)$ is well known, consisting of a

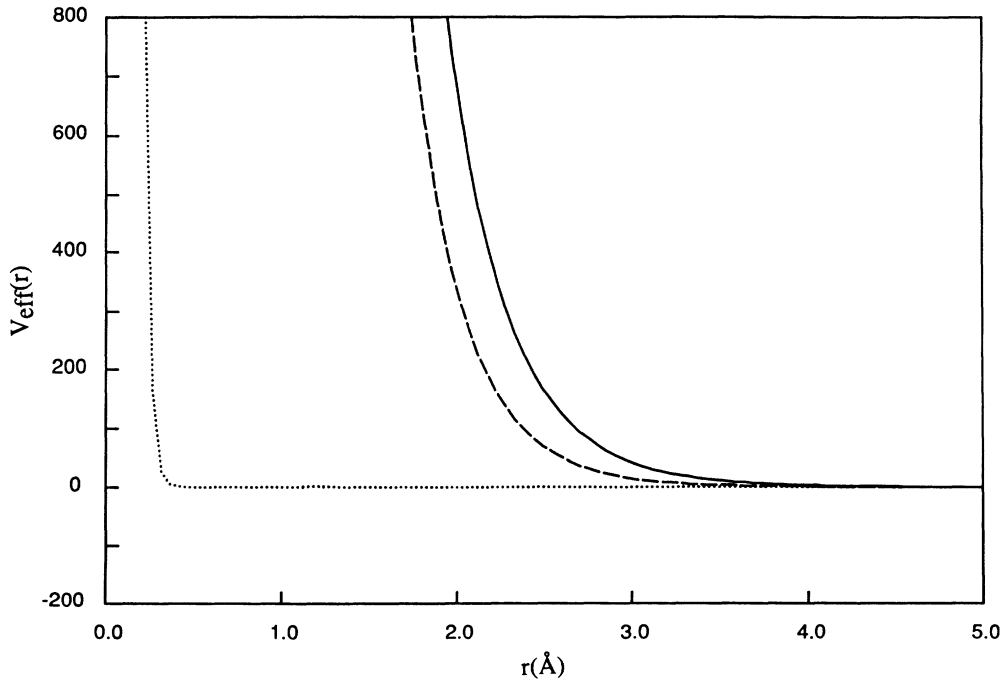

FIG. 5. $V_{\text{eff}}(r)$ given by electronic and boson screening according to Eqs. (9) and (10). (i) Electronic screening alone, with $K_s=2.40$ Å^{-1}, corresponding to a Fermi surface density of states $N(\varepsilon_F)=0.47$ states/(eV Pd) for PdH (Ref. 11) (——). (ii) Electron and boson screening, with $K_s=2.76$ Å^{-1}, corresponding to $\langle(\delta n)^2\rangle=0.2\times10^{-3}$ (— — —). (iii) Electron and boson screening, with $K_s=16.41$ Å^{-1}, corresponding to $\langle(\delta n)^2\rangle=0.29\times10^{-1}$ (· · · ·) (Table II).

short-range screening charge distribution which can to first order be described in the Thomas-Fermi model, and a long-range oscillatory part deriving from the singularities of $\epsilon(\mathbf{k})$.[20] To evaluate the effects of boson screening on diffusion and on tunneling through the Coulomb barrier; it suffices to consider only the short-range repulsive part of $V_{\text{eff}}(r)$ to obtain order of magnitude estimates. We can obtain an upper bound on the screening of this by taking $\hat{\chi}_d(\mathbf{k})$ independent of $\mathbf{k}$, for all $\mathbf{k}$, and combining this with the Thomas-Fermi electronic screening result

$$\lim_{\mathbf{k}\to 0}\chi_e(\mathbf{k})=\frac{\partial n}{\partial\mu}=N(\varepsilon_F)\ . \tag{8}$$

This yields a total screened Coulomb potential between two deuterons

$$V_{\text{eff}}(r)=\frac{e^2}{r}e^{-K_s r} \tag{9}$$

with

$$K_s^2=4\pi e^2N(\varepsilon_F)+4\pi e^2\beta\langle(\delta n)^2\rangle=K_e^2+K_d^2\ . \tag{10}$$

Taking a typical value of $N(\varepsilon_F)=0.47$ states/(eV Pd) for PdH,[11] gives $K_e=2.40$ Å^{-1}. The repulsive short-range part of the potential is shown in Fig. 5, for electronic screening alone (solid line) and with additional boson screening deriving from $\langle(\delta n)^2\rangle=0.2\times10^{-3}$ (dashed line) and $\langle(\delta n)^2\rangle=0.29\times10^{-1}$ (dotted line). These values of $\langle(\delta n)^2\rangle$ are appropriate for stoichiometric PdD with coherent motion in the ($N=4$)-site cluster, with (a) $t\sim1$ meV, $U\sim1$ eV, $k_BT=25$ meV and (b) $t\sim25$ meV, $U\sim2.5$ eV, $k_BT\sim25$ meV (third and fourth rows, Table II). Since the short-range part of the H-H (D-D) potential is an important factor in concentration dependence of mobilities at high concentrations,[1] such a concentration-dependent boson screening mechanism will be significant for deuterium mobilities at high concentrations. The differences seen between fermion and boson fluctuations in Figs. 2–4 clearly suggest that the deuterium mobility will be anomalously high amongst the three hydrogen isotopes. The effects of boson screening on the long-range part of $V(r)$ will be investigated in future work.

Note that the self-consistent procedure outlined above amounts to replacing $\hat{\chi}_d(k)$ by its value at an intermediate length scale, and also includes some degree of polarization of the electronic environment by the deuterons, because of the use of the screened Hubbard U parameter. Thus although its use down to the nuclear region is an extrapolation, it does not imply a completely uniform background and so does not obviously violate the Born-Oppenheimer approximation.

IV. ENHANCEMENT OF COLD FUSION RATES BY BOSON SCREENING

The thermally averaged fusion rate for the reaction $d+d\rightarrow\text{He}^3+n$ is given by

$$\Lambda=\frac{1}{a^3}\langle A2\pi\eta e^{-B}\rangle \tag{11}$$

with

$$B(E)=\frac{2}{\hbar}(2\mu_{dd})^{1/2}\int_{r_0}^{r_1}[V_{\text{eff}}(r)-E]^{1/2}dr\ . \tag{12}$$

Here $A=2\times10^{-16}$ cm^3 s^{-1} is the nuclear-reaction-rate constant,[9] $\eta=e^2/\hbar v$ and B is the semiclassical WKB tunneling integral for the screened Coulomb potential. Use of the WKB approximation in (11) yields a lower limit to the rate. The barrier-penetration factor depends both on the relative kinetic energy E, which depends on the vibrational state, and on the screened potential $V_{\text{eff}}(r)$. As noted earlier, $V_{\text{eff}}(r)$ would also be vibrational state dependent in a more detailed calculation. Since over the kinetic energy range possible in these circumstances ($0<E<1.0$ eV) little change in $B(E)$ is obtained,[21] we restrict our estimates here to a single relative kinetic energy and consider only the range of $V_{\text{eff}}(r)$ introduced by temperature-dependent density fluctuations within a single band of vibrational states, as given in Table II. Thus we evaluate the room-temperature fusion rate with

$$\Lambda=\frac{A2\pi\eta}{a^3}e^{-B} \tag{13}$$

where B [Eq. (12)] is evaluated at room temperature, $E=298$ K. Λ is very weakly dependent on the relative velocity v and we approximate this by the velocity of a deuterium species in the ground vibrational state of the octahedral Pd site, $v=2\times10^5$ cm s^{-1}, derived from a vibrational frequency of $\omega_D=42$ meV.[1] The $1/a^3$ factor in Eqs. (11) and (13) derives from the density dependence of the rate. Since the deuterium tunnels between adjacent sites, and spends most time in the interstitial sites, we take a^3 to be the volume of an interstitial octahedral hole, rather than the reciprocal of the actual density in PdD. With a lattice constant of 3.89 Å for fcc Pd, this yields $a^3=0.774$ Å^3, from consideration of packing of hard spheres. B was then evaluated by numerical integration.

Table III contains the fusion rates resulting from adding boson screening to the normal electronic screening, with the range of values of $\langle(\delta n)^2\rangle$ shown in Figs. 2–4 and Table II. For comparison we show also the fusion rate obtained with electron screening alone for values of K_s derived from (i) the density of states of PdD, $N(\varepsilon_F)=0.47$ states/(eV Pd) (Ref. 11) ($K_s=2.40$ Å^{-1}), and (ii) the density of states of pure Pd, $N(\varepsilon_F)\sim2.27$ states/(eV Pd) (Ref. 11) ($K_s=5.28$ Å^{-1}).

The value $\Lambda=4\times10^{-99}$ s^{-1}, obtained with the density of states appropriate to stoichiometric PdD, is in agreement with the recent calculations of Burrows,[21] and is significantly less than that predicted for fusion in gas-phase D_2 molecules.[8] This is a consequence of the low electron density at the Fermi surface in PdD, rather than of the delocalized nature of the metallic electrons, as is evident from the increase to $\Lambda=8\times10^{-65}$ s^{-1} when the Fermi surface density of states is set equal to that of pure Pd.

The results shown in Tables II and III show that the fusion rates are critically sensitive both to the ratios U/t and k_BT/t, to the deuterium concentration, and to the range of coherence, i.e., N. The fusion rates are plotted as a function of $\langle(\delta n)^2\rangle$ in Fig. 6. For stoichiometric PdD, with the large coherence range of the $N=4$ cluster

TABLE III. Fusion rate Λ [Eq. (13)] expressed as the rate per d^+-d^+ pair per second, calculated as a function of the inverse screening length K_s [Eq. (10)] for stoichiometric PdH and PdH_2 over the range of boson screening contributions $\langle(\delta n)^2\rangle$ shown in Table II.

Screening entity	$\langle(\delta n)^2\rangle$	K_s (Å^{-1})	B	Λ (s^{-1})
e^-	0	2.40	259.4	4.14×10^{-99}
e^-	0	5.28	175.7	8.67×10^{-65}
e^-,d^+	1.00	95.34	40.2	6.22×10^{-6}
e^-,d^+	0.16	38.19	64.7	1.44×10^{-16}
e^-,d^+	0.11	31.71	71.2	2.22×10^{-19}
e^-,d^+	0.10	30.24	72.9	3.94×10^{-20}
e^-,d^+	0.36(−1)	18.25	94.3	1.99×10^{-29}
e^-,d^+	0.33(−1)	17.48	96.4	2.48×10^{-30}
e^-,d^+	0.30(−1)	16.69	98.7	2.52×10^{-31}
e^-,d^+	0.29(−1)	16.41	99.5	1.08×10^{-31}
e^-,d^+	0.18(−2)	4.70	186.2	2.51×10^{-69}
e^-,d^+	0.12(−2)	4.08	199.7	3.45×10^{-74}
e^-,d^+	0.62(−3)	3.39	218.8	1.67×10^{-83}
e^-,d^+	0.59(−3)	3.34	220.5	3.35×10^{-84}
e^-,d^+	0.40(−3)	3.07	229.8	2.92×10^{-88}
e^-,d^+	0.20(−3)	2.76	242.2	1.27×10^{-93}
e^-,d^+	0.12(−4)	2.43	257.9	1.97×10^{-100}
e^-,d^+	0.40(−5)	2.41	258.8	6.89×10^{-101}

and periodic boundary conditions, there is a critical jump in fusion rate as U/t decreases from 10^3 to 10^2. If coherent motion is limited to $N=2$ clusters, with no periodic boundary conditions (the minimal range), then for stoichiometric PdD, the fusion rate is less than 10^{-83} s^{-1} for all ratios U/t, except for $U/t=10^2$, $k_BT=25t$, for which $\Lambda\sim10^{-30}$ s^{-1}. The situation is very different, however, at concentrations corresponding to the dihydride. Here the $N=4$ cluster yields fusion rates greater than 10^{-20} s^{-1} for $U/t=10^2$, which would be readily detectable, while the $N=2$ cluster yields maximum fusion rates of 10^{-29} s^{-1} here, similar to those obtained for PdD.

When one considers what realistic values of the Hubbard parameters are, then the conclusions as to feasibility of fusion rates of $\Lambda\geq10^{-23}$ s^{-1} in stoichiometric PdD

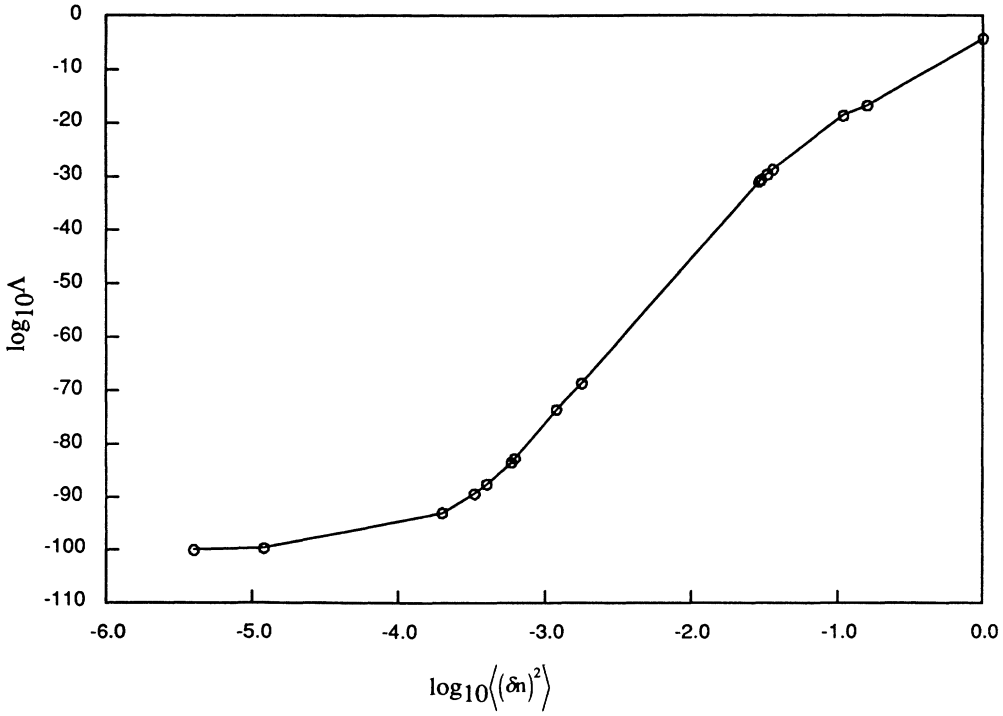

FIG. 6. $\log_{10}\Lambda$ as a function of $\log_{10}\langle(\delta n)^2\rangle$ for the reaction $d+d\rightarrow{}^3\mathrm{He}+n$. Λ is evaluated with Eqs. (9)–(12). Circles indicate the points obtained with the values in Tables II and III. [An additional point for $\langle(\delta n)^2\rangle=1.0$ is shown for reference.]

(Refs. 5 and 6) appear negative. To obtain a value of Λ greater than 10^{-25} s^{-1} requires $\langle(\delta n)^2\rangle$ greater than 6×10^{-2} (Fig. 6). Our calculations show that this is not possible with realistic values of U and t, if only $N=2$ clusters are involved. The rate increases considerably for the larger clusters. Thus, with the long-range coherent motion of the $N=4$ cluster and periodic boundary conditions, the estimates $t\sim25$ meV, $U\sim2.5$ eV, yield fusion rates $\Lambda\sim10^{-31}$ s^{-1} at room temperature. It is instructive also to compare these estimates with the rigorous upper bound of $\Lambda\sim10^{-47}$ s^{-1} at $T=0$, obtained by Leggett and Baym.[14] The $T=0$ results obtained within our approximate Hamiltonian for the stoichiometric PdD species can be seen from Tables II and III to be well below this bound, for all values of parameters except $U/t=10^2$ in the $N=4$ cluster. This implies that $U/t>10^2$ in the ground vibrational state, as expected (see earlier discussion of realistic parameter values). Finite-temperature rate enhancements would therefore derive from population of excited vibrational states with such smaller ratios of U/t. The finite-temperature values are larger and, for a range of parameters studied here, considerably exceed the zero temperature bound. These values of the parameters are appropriate to motion in excited vibrational states, and represent very optimistic estimates. Moreover, the data presented in Figs. 2 and 3 and Tables II and III do indicate that the rates will be very sensitive to the exact value of U for $U/t<10^3$. Note that the first row of Table II, corresponding to $t\sim1$ meV, $U\sim100$ meV, yields $\Lambda\sim10^{-19}$ s^{-1}. Such a low value of U appears unlikely from what is currently known about the energetics.[17–19] Thus we conclude that, given what is currently known about the dynamics of deuterium in Pd, fusion rates of 10^{-23} s^{-1} are not possible in stoichiometric PdD unless there is an unusually low value of U.

With the dihydride, PdD_2, our results indicate that fusion rates of 10^{-23} s^{-1} [requiring $\langle(\delta n)^2\rangle>6\times10^{-2}$] may be possible with realistic values of U and t at room temperature, provided that coherent motion occurs within clusters larger than $N=2$, e.g., line 2 in Table II. This would be somewhat unusual in a bulk metal at room temperature, the only unambiguous independent experimental observation of true long-range coherent motion being for hydrogen on metal surface at lower temperatures.[2,3] However, we emphasize that a cluster such as the $N=4$ cluster of octahedral sites in fcc palladium in which every site is connected to every other by nearest-neighbor separation requires that coherence be maintained only over distances of ~3.89 Å, which may be possible in excited vibrational states.

Finally, we conclude that boson screening induced by finite-temperature coherent dynamics can certainly induce huge enhancements over the $d+d$ fusion rates in gas-phase molecular D_2,[8] and also over the $T=0$ rates in metallic Pd.[14] The additional screening mechanism introduced by finite-temperature boson fluctuations has significant effects even for small values of the fluctuations, and is very sensitive to both concentration and the relative magnitudes of the Hubbard parameters t and U. We note that the boson screening mechanism described here would also be effective in enhancing other fusion reactions in the metal, provided the deuterium concentration was high enough. In this analysis of bosonic collective effects, we have (i) assumed an approximate Hamiltonian, (ii) obtained the effective interaction potential within linear response, and calculated the barrier penetration within the WKB approximation, and (iii) treated the dielectric constant $\epsilon(k)$ as a constant. To obtain more accurate estimates of finite-temperature rates, each of these approximations must be critically examined and possibly superseded. More precise calculations of the parameters t and U, and of the effective dielectric constant, Eq. (6), will be especially useful. Although the calculations made here do not quantitatively support the recent experimental claims of $\Lambda\sim10^{-23}$ s^{-1}, nevertheless, the magnitude of the enhancements obtained here with realistic but still approximate values of t and U, and the strong concentration dependence seen for PdD_x, $x>1$, suggest that further exploration of environments favoring collective coherent motion will be very interesting.

ACKNOWLEDGMENTS

I thank R. A. Harris for critical reading of the manuscript. This research has been supported in part by the Petroleum Research Fund, administered by the American Chemical Society, and in part by the Office of Naval Research. Computing support from the Center for Advanced Materials at Lawrence Berkeley Laboratory is gratefully acknowledged.

[1] Y. Fukai and H. Sugimoto, Adv. Phys. **34**, 263 (1985); extensive references to recent theoretical and experimental studies are given here.

[2] S. C. Wang and R. Gomer, J. Chem. Phys. **83**, 4193 (1985); R. DiFoggio and R. Gomer, Phys. Rev. B **25**, 3490 (1982).

[3] K. B. Whaley, A. Nitzan, and R. B. Gerber, J. Chem. Phys. **84**, 5181 (1986).

[4] K. B. Whaley and L. M. Falicov, J. Chem. Phys. **87**, 7160 (1987).

[5] M. Fleischman, S. Pons, and M. Hawkins, J. Electroanal. Chem. **261**, 301 (1989).

[6] S. E. Jones, E. P. Palmer, J. B. Czirr, D. L. Decker, G. L. Jensen, J. M. Thorne, S. F. Taylor, and J. Rafelski, Nature (London) **338**, 737 (1989).

[7] For a review of other experimental work, see abstracts in Bull. Am. Phys. Soc. **34**, 1859 (1989).

[8] C. D. Van Siclen and S. E. Jones, J. Phys. G **12**, 213 (1986); S. E. Koonin and M. Nauenberg, Nature (London) **339**, 690 (1989) (the values obtained here by more accurate calculations, predict $\Lambda\sim10^{-64}$ s^{-1}).

[9] J. D. Jackson, Phys. Rev. **106**, 330 (1957).

[10] For a recent review of muon-catalyzed fusion, see S. E. Jones, Nature (London) **321**, 127 (1986).

[11] C. T. Chan and S. G. Louie, Phys. Rev. B **27**, 3325 (1983); D.

A. Papaconstantopoulos, B. M. Klein, J. S. Faulkner, and L. L. Boyer, *ibid.* 2784 (1978); A. C. Switendick, Ber. Bunsenges. Phys. Chem. **76**, 535 (1972).

[12]H. Wipf, in *Hydrogen in Metals II,* Vol. 29 of *Topics in Applied Physics,* edited by G. Alefeld and J. Völkl (Springer-Verlag, Berlin, 1978), Chap. 7.

[13]G. Sicking, Ber. Bunsenges. Phys. Chem. **76**, 790 (1972).

[14]A. J. Leggett and G. Baym, Phys. Rev. Lett. **63**, 191 (1989).

[15]L. M. Falicov and R. H. Victora, Phys. Rev. B **30**, 1695 (1984).

[16]E. M. Lifshitz and L. P. Pitaevskii, *Statistical Physics I* (Pergamon, Oxford, 1980).

[17]Z. Sun and D. Tománek, Phys. Rev. Lett. **63**, 59 (1989); J. W. Mintmire, B. I. Dunlap, D. W. Brenner, R. C. Mowrey, H. D. Lacouceur, P. P. Schmidt, C. T. White, and W. E. O'Grady, Phys. Lett. A **138**, 51 (1989).

[18]P. Nordlander, J. K. Nørskov, F. Besenbacher, and S. M. Myers, Phys. Rev. B **40**, 1990 (1989).

[19]O. B. Christensen, P. D. Ditlevsen, K. W. Jacobsen, P. Stoltze, O. H. Nielsen, and J. K. Nørskov, Phys. Rev. B **40**, 1993 (1989).

[20]S. Dietrich and H. Wagner, Z. Phys. B **36**, 121 (1979); H. Horner and H. Wagner, J. Phys. C **7**, 3505 (1974); V. G. Vaks, N. E. Zein, V. G. Orlov, and V. I. Zinenko, J. Less-Common Met. **101**, 493 (1984); K. H. Lau and W. Kohn, Surf. Sci. **75**, 69 (1978).

[21]A. Burrows, Phys. Rev. B **40**, 3405 (1989).